Mechanical and Physical Properties of Dispersion-Strengthened Iron

Mechanical and Physical Properties of Dispersion-Strengthened Iron*

Yûnoshin IMAI and Tôru MIYAZAKI

The Research Institute for Iron, Steel and Other Metals

(Received October 8, 1963)

Synopsis

The dispersion-strengthening phenomenon in iron was studied by using fine powders of alumina, magnesia and silica as dispersing particles. Observations were carried out of micrographs, hardness, creep rupture and thermal expansion. Cu base dispersion-strengthened alloys were also examined for reference. The results obtained were as follows: (1) In iron alloys alumina was most effective and silica was least. (2) Growth of particles during heating at high temperature may be due to the existence of wustite. (3) The less the expansion coefficient, the stronger the effect of dispersion strengthening.

I. Introduction

Aluminium, copper, silver and nickel base dispersion-strengthened materials have been studied by many workers.[1–4] There are, however, few reports on dispersion-strengthened iron.[5–7] So, in the present work, several mechanical properties and thermal expansion of dispersion-strengthened irons were studied.

II. Experimental method

1. Preparation of specimen

Hägänes iron powder (subsieved powder) and commercial copper powder (less than about 20μ in diameter) as base metal, and α-alumina, magnesia and silica as dispersed particle were used.

The oxide powders were pulverized in a ball mill for 500 hours. The powders were mixed in water and finer particles were separated by decantation. These oxide powders being of almost uniform size were finer than about 1μ in diameter.

For the preparation of specimens, the metal powder and 5, 10 and 15 volume per cent of oxides were mixed in a ball mill with benzol for 70 hours, reduced in dry

* The 1100th report of the Research Institute for Iron, Steel and Other Metals.

(1) N.J. Grant and O. Preston, J. of Metals, **9** (1957), 349.
(2) C.G. Goetzel, J. of Metals, **11** (1959), 189, 276.
(3) M.S. Ali and V.A. Philips, Trans. AIME, **215** (1959), 340.
(4) R.H. Seebohn and J.W. Martin, Metallurgia, **61** (1960), 163.
(5) A. Gatti, Trans. AIME, **218** (1960), 437.
(6) Y. Imai and H. Hirotani, Sci. Rep. RITU, **A 12** (1960), 168.
(7) W. Jellinghaus and T. Shuin, Stahl u. Eisen, **78** (1958), 419.

hydrogen stream at 600°C for 2 hours, and the powder mixtures were compressed and sintered. In the compression the hydrostatic pressure was 5 t/cm^2 for iron-oxide powders and 2t/cm^2 for copper-oxide powders.

Green compacts of iron and copper base were sintered in dry hydrogen stream at 1360°C and 1000°C, respectively. The sintered specimen was improved by repressing at room temperature followed by the so-called step sintering. The sintered compact was of 10×10 mm in width and 100 mm in length, and maximum density ratio of the specimen prepared was 0.98.

III. Experimental results

1. Microphotographs

Microphotographs of dispersion-strengthened irons containing each 10 vol. per cent of Al_2O_3, MgO and SiO_2 are shown in Phots. 1(A), (B) and (C), respectively, in which oxide particles are seen as black points. In (A) the distribution of particles is more regular and finer than in (B) and (C).

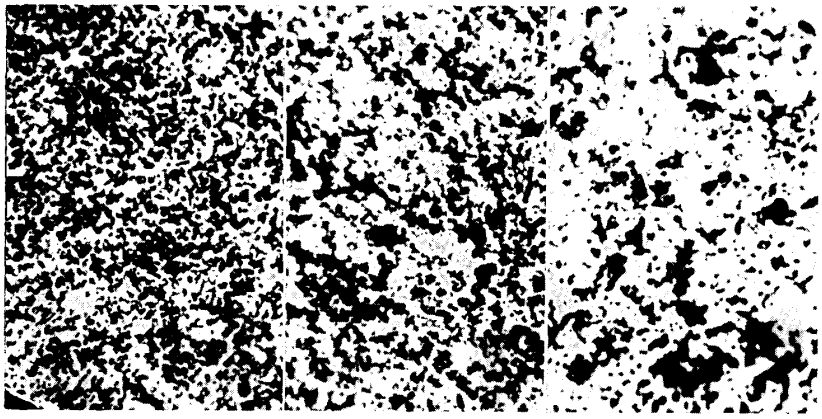

(a) (b) (c) ×1000

Phot. 1. Microphotographs of dispersion-strengthened irons.
(A) Fe-10vol.%Al_2O_3 (B) Fe-10vol.%MgO (C) Fe-10vol.%SiO_2

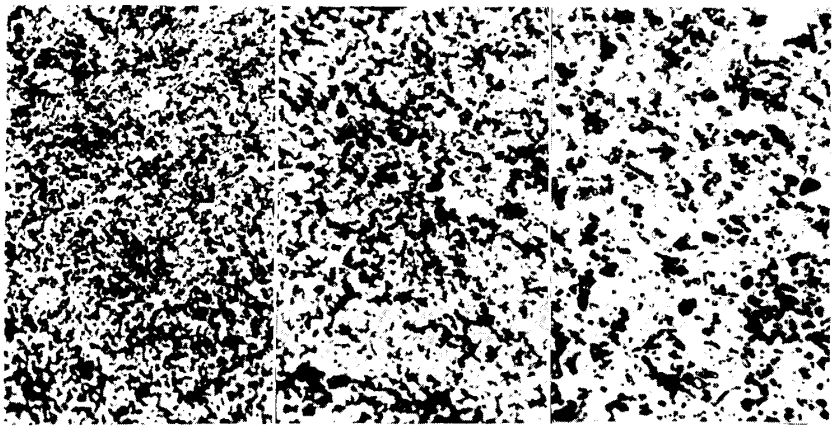

(a) (b) (c) ×1200

Phot. 2. Microphotographs of dispersion-strengthened coppers.
(A) Cu-5vol.%Al_2O_3 (B) Cu-5vol.%MgO (C) Cu-5vol.%SiO_2

Phots. 2 (A), (B) and (C) are microphotographs of dispersion-strengthened coppers containing each 5 vol. per cent of Al_2O_3, MgO and SiO_2, respectively. The oxides in copper-alumina alloys are distributed most evenly, while in copper-silica alloys the distribution is most uneven. This difference may arise from the difference in physical and chemical properties of these oxides, because in these alloys the size and the size distribution of oxide particles before sintering were almost equal as mentioned above, that is, during sintering at high temperatures the growth of these oxides might take place corresponding to the thermal stability of respective oxides.

2. Growth of dispersed particles

It is considered that Al_2O_3, MgO and SiO_2 are each insoluble in iron or copper in solid state even at high temperatures, but actually these coagulate during heating at the sintering temperature.[8,9] The growth of oxide particles were observed more markedly in vacuum rather than in the stream of dry hydrogen in iron compacts sintered at 1360°C for 4 hours.

In order to study the nature of the coagulated oxide in the pure iron compact sintered in dry hydrogen stream, the oxides were electrolytically separated under the following condition.

Electrolyte: $FeSO_4 \cdot 7H_2O$ 40 g,
$(NH_4)_2SO_4$ 30 g,
$FeCl_2 \cdot 4H_2O$ 20 g,
and
$(NH_4)_2HC_6H_5O_7$ 3 g,

were dissolved in 1*l* of water. The electrolyte was kept at pH 5 during electrolysis by adding H_2SO_4 or NH_4OH. Current density was 10 mA/cm_2. The electrolytic residue was filtered, dried and analyzed by the X-ray. Lattice spacings, d, obtained are shown in Table 1. Wustite, FeO, is distinctly observed in the residue of the sintered pure iron.

Table 1. X-ray diffraction analysis of electrolytical residue of sintered pure iron

Line spacing (mm)	Lattice spacing (Ä)	Materials
39.5	5.52	$FeSO_4$, $3H_2O$
46.0	4.90	$FeSO_4$, $7H_2O$
67.0	3.40	$FeSO_4$, $3H_2O$
88.9	2.47	FeO
103.5	2.14	FeO
111.9	1.99	$FeSO_4$, $3H_2O$
152.6	1.51	FeO

FeKα.

The presence of $FeSO_4$ may be due to the contamination of electrolyte. When FeO, alumina, silica and magnesia co-exist, the compound $(FeO)_x(SiO_2)$ or $(FeO)_x$

(8) N.J. Grant and N. Komatsu, Trans. AIME, **224** (1962), 705.
(9) Dromsky, F.V. Lenel and G.S. Ansell, Trans. AIME, **224** (1962), 236.

(Al_2O_3) may appear during sintering at high temperatures because of FeO having a slight solid solubility in Fe at that temperature, and if the volume of FeO increases further, there appears the binary eutectic of FeO-Al_2O_3, FeO-MgO or FeO-SiO_2 having far lower melting point than that of each of oxides; that is, the melting points of SiO_2 and Al_2O_3 are 1728°C, 2015°C, respectively, that of eutectic FeO-SiO_2 is 1178°C and that of FeO-Al_2O_3 is 1480°C (Al_2O_3 57 per cent, FeO 43 per cent), although a complete phase diagram is yet unknown. Therefore, the eutectic mixture of FeO-SiO_2 melts completely and that of FeO-Al_2O_3 will partially melt at the sintering temperature, 1360°C. Consequently, in the case of dispersion-strengthened iron containing FeO, the growth of oxide particles will naturally take place.

The microphotographs of dispersion-strengthened irons containing alumina and sintered in dry hydrogen stream and in vacuum (10^{-3} mm Hg) are shown in Phots. 3(A) and (B), respectively. Coarser dispersion is observed in the compact sintered in vacuum than that sintered in dry hydrogen stream.

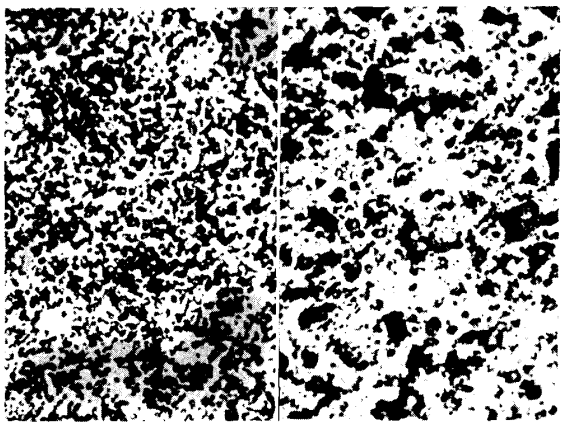

(A) (B)

Phot. 3. Growth of alumina on the alloy sintered in dry hydrogen stream (A) and in vacuum (B).

From the experimental results it can be said that FeO contained in green compacts with alumina can be reduced more incompletely during sintering in vacuum (10^{-3} mm Hg) than in dry hydrogen stream. Consequently, alumina particles are larger in the compact sintered in vacuum than that sintered in hydrogen as shown in Phots. 3 (A) and (B). So the growth of oxide particles may be due to the existence of wustite, viz. the more the oxygen is contained in the alloy, the larger the particle size becomes.

3. Hardness

Fig. 1 shows the hardness at room temperature after annealing of cold-worked dispersion-strengthened irons containing Al_2O_3, MgO or SiO_2, respectively. Specimens were cold-worked by 60 per cent by compression. As shown in Fig. 1 pure iron softens rapidly by annealing at recrystallization temperature of about

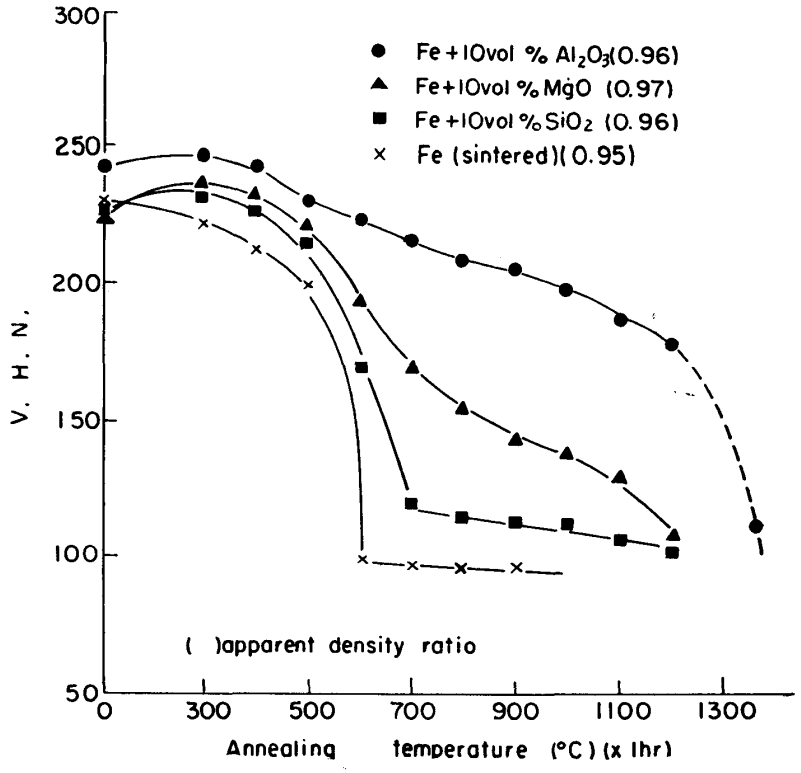

Fig. 1. Hardness at room temperature of cold-worked dispersion-strengthened irons after annealing.

600°C, while dispersion-strengthened irons, especially Fe-Al_2O_3 alloy, do not soften by annealing at recrystallization temperature and also at A_3 transformation point.[6][10]

Numbers in round brackets show apparent density ratio. The porosity affects mechanical properties of specimen. The change in hardness after annealing of cold-worked specimens with various densities of Fe-Al_2O_3 alloy is shown in Fig. 2. The distributions of oxide particles in these specimens were almost equal to one another. As shown in Fig. 2 dispersion-strengthened irons with density ratio bellow 0.90 soften rapidly by annealing at the recrystallization temperature.

Next, the relation between hardness and line broadening of X-ray diffraction pattern was observed. Fig. 3 shows the change in the lattice distortion due to the cold working of 60 per cent by compression and the change after heating for 1 hour by integrated breadth from the X-ray diffraction patterns. In Fig. 3 "S" refers to "as-sintered alloy" and C.W. "cold worked alloy". The line broadening of Fe-Al_2O_3 alloy does not recover to the level of that of the sintered specimen by heating at recrystallization temperature and even at the A_3 transformation point.

Broadening of X-ray diffraction line is due to lattice distortion caused by cold working, and disarranged reflexion is also caused by break down of metal grains.

(10) Y. Imai and T. Miyazaki, Sci. Rep. RITU, **A14** (1962), 146.

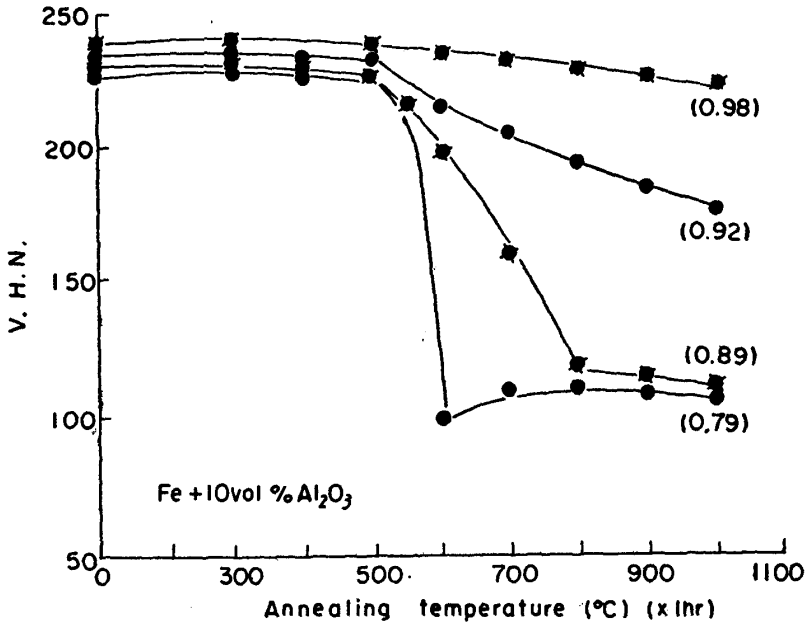

Fig. 2. Change of annealing hardness with apparent density ratio of dispersion-strengthened irons.

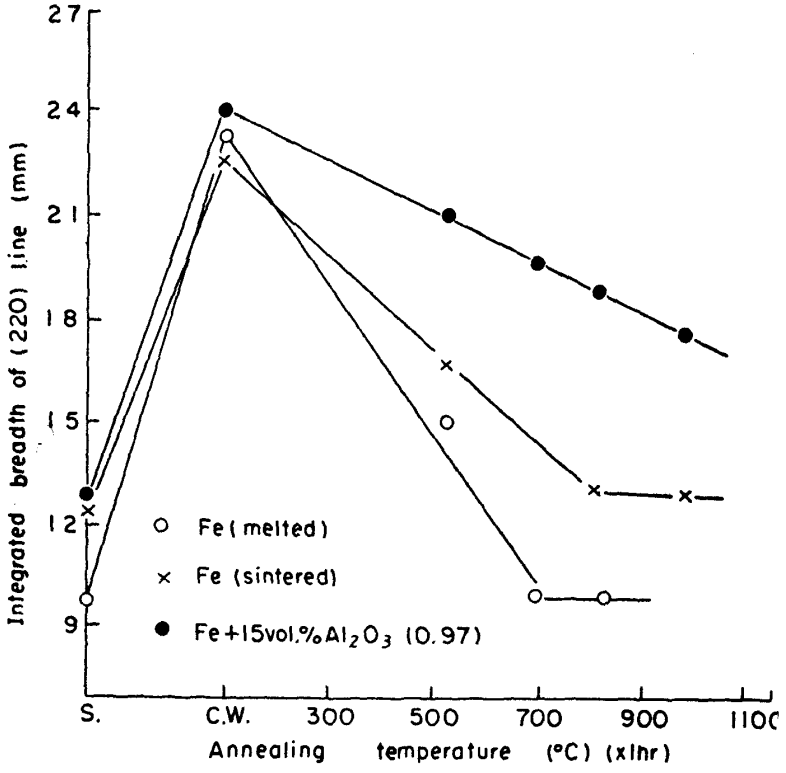

Fig. 3. Integrated breadth of (220) line of dispersion-strengthened irons.

Therefore, in order to estimate the lattice distortion from the broadening of diffraction line, it is necessary that the grain size must be unchanged after any treatment such as cold working and heating. As reported[11] the broadenings are caused not by fine grains, but lattice distortion.

Actually, in the present work, the grain size was not changed by each treatment, since the specimens were prepared by the process of the stepped sintering, viz. sintering – cold working at room temerpature. Sub-grains formed by cold working also have an effect on the broadening of diffraction lines. However, even if sub-grains are broken down by cold working, the broken grains will grow up to a size which does not affect line broadening by heating above 400°C. From these circumstances, it is assumed that the grain size does not change throughout these treatments, and hence the difference in integrated breadths between as-sintered and cold-worked states in Fig. 3 may be due to lattice distortion caused by cold working. Consequently, dispersion-strengthened iron, Fe–15 vol. per cent Al_2O_3, retains strains caused by cold working even if it is heated above the A_3 point of iron as reported.[6,10,11] It is noteworthy that the dispersion-strengthened iron retains internal strains caused by cold working which are not relieved by recrystallization and even by the A_3 transformation.[6,9,10]

It is not clear whether a small difference between the integrated breadth of

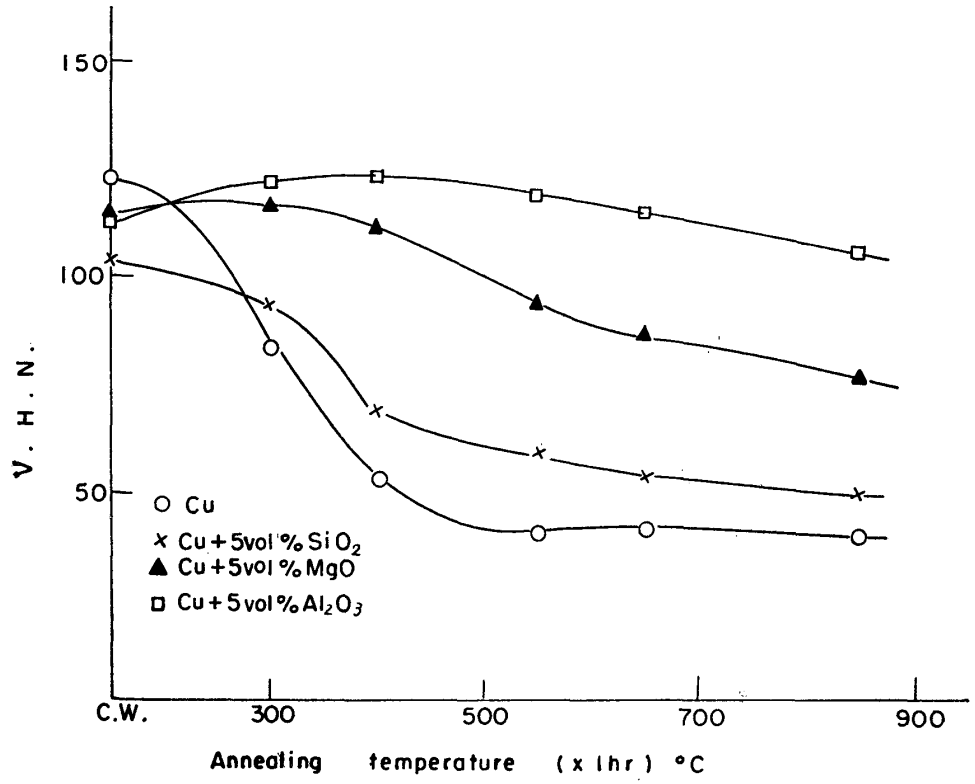

Fig. 4. Relation between room temperature hardness and annealing temperature for 1 hour for Cu base dispersion-strengthened alloys.

(11) Y. Imai and H. Hirotani, *Powder Metallurgy*, 1960 (New York), 359.

melted pure iron and that of dispersion-strengthened iron of as-sintered state is due to line broadening caused by the break down of grains of dispersion-strengthened iron or it is due to internal strains caused by difference between thermal expansion of matrix and oxide particles.

Fig. 4 shows the relation between hardnesses at room temperature and annealing temperatures of 60 per cent cold-pressed dispersion-strengthened copper. In this case the hardness of Cu-Al_2O_3 alloy is larger than the other two, and that of pure copper is the least.

Hot hardness of cold-worked dispersion-strengthened iron, Fe-Al_2O_3, Fe-MgO and Fe-SiO_2 are shown in Fig. 5. Room temperature hardness shown by dotted lines is the same as that in Fig. 1 and full line refers to hot hardness. Dispersion-strengthened iron shows, to be sure, higher hardness than pure iron at high temperatures.

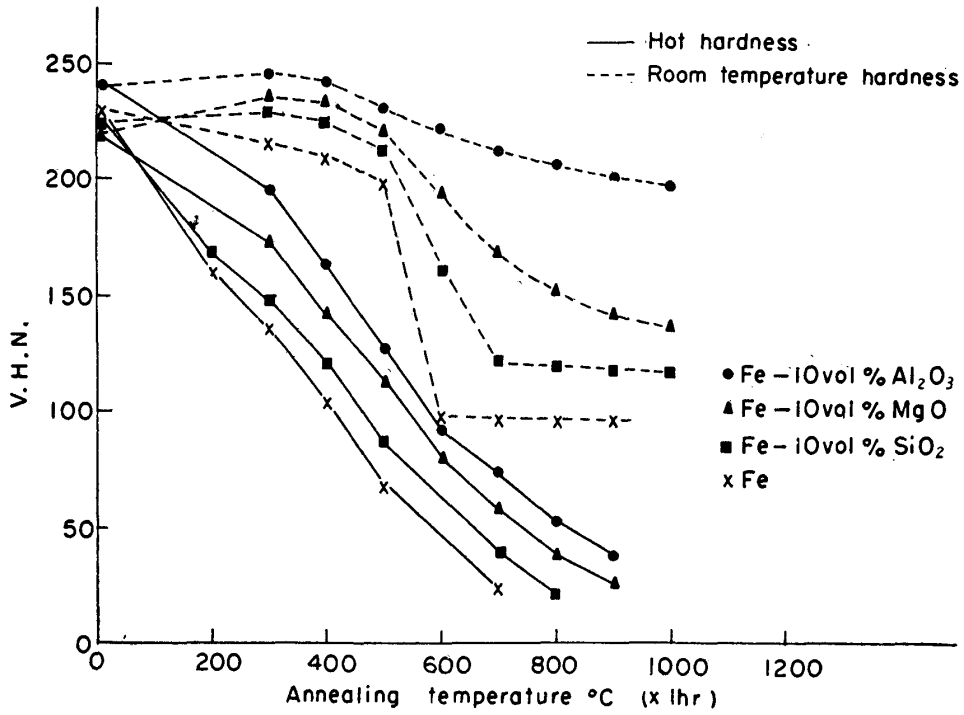

Fig. 5. Hot hardness and room temperature hardness of cold-worked dispersion-strengthened iron.

4. Creep rupture test

Fig. 6 shows creep rupture strength of dispersion-strengthened irons with equal density and similar alumina distribution, and Fig. 7 shows that with almost equal density but with different sizes of alumina particles. In Fig. 7 oxide mean free path measured by linear analysis in specimens (a), (b), (c) and (d) are about 1.7μ, 0.6μ, 0.3μ and 0.2μ, respectively. From the results it can be seen that the creep rupture strength is affected by the density of specimen or by the distribution of alumina. A logarithmic relation between alumina distribution and creep rupture

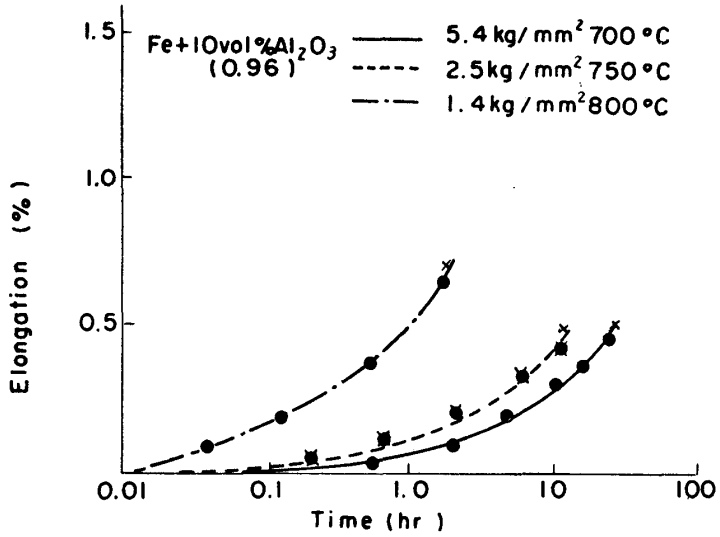

Fig. 6. Creep rupture behaviors of Fe−10vol.%Al_2O_3 (0.96) with equal density and similar alumina distribution.

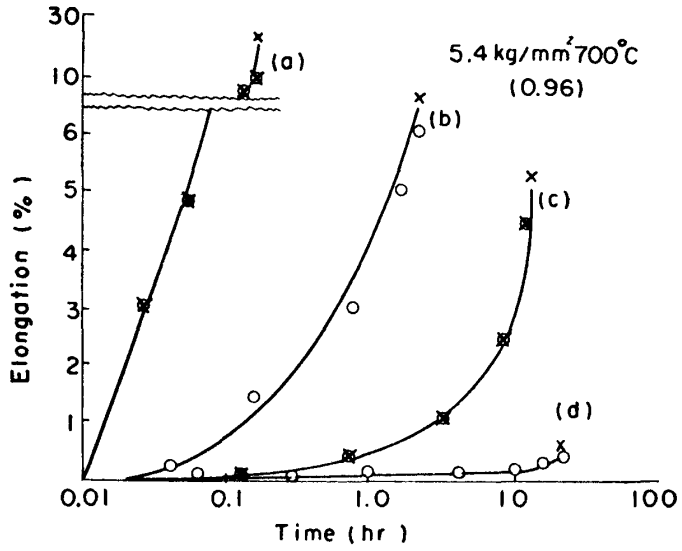

Fig. 7. Creep rupture behaviors of Fe-10vol.%Al_2O_3 (0.96) with various alumina distribution.

time is shown in Fig. 8. Here specimens having different spacings of Al_2O_3 were obtained by different heating times at 1360°C, so these specimens have almost the same volume per cent of Al_2O_3 but different sizes of Al_2O_2 particles.

5. Thermal expansion

It has been known that thermal expansions of dispersion-strengthened alloys are smaller than those of melted pure metals. For example, the expansion coefficient of SAP is about 20×10^{-6}, while that of Y-alloy which is aluminium base alloy is 24×10^{-6}.

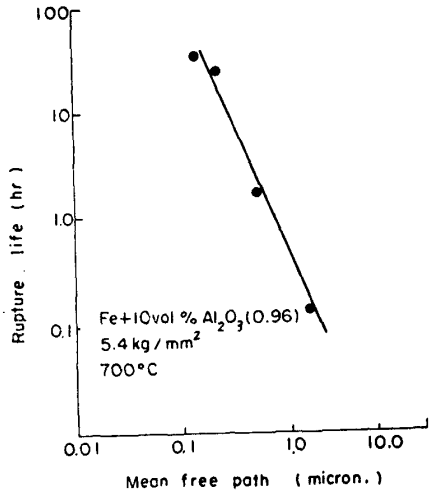

Fig. 8. Logarithmic relation between rupture life and average mean free path on Fe-10vol.%Al_2O_3 for 5.4kg/mm² at 700°C.

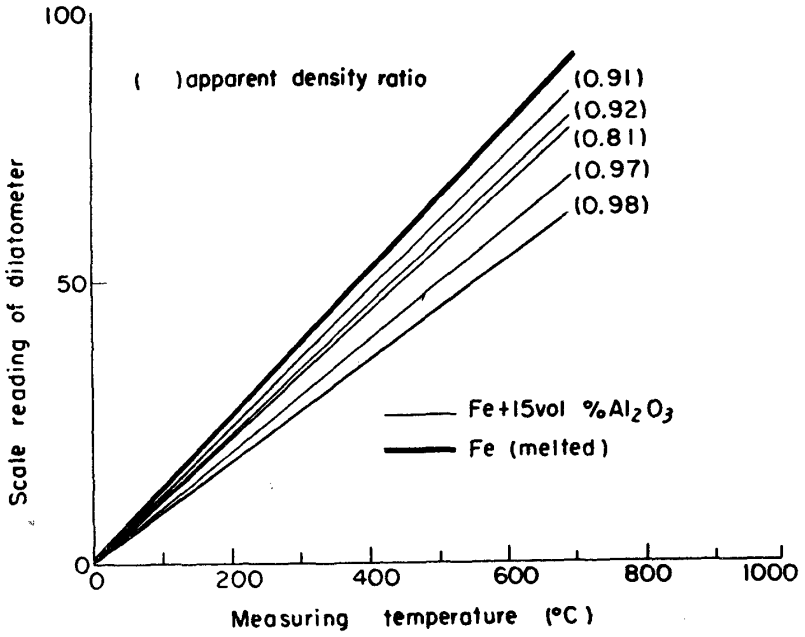

Fig. 9. Thermal expansion of dispersion-strengthened irons.

Fig. 9 shows thermal expansion of sintered Fe-Al_2O_3 alloy with various apparent densities, which was measured at 500~700°C on heating. From these results it will be seen that the thermal expansion of sintered alloys is smaller than that of pure iron. These relations are more clearly shown in Fig. 10. The coefficients of thermal expansion of the sintered alloys increase as the apparent density ratio increases up to about 0.90 and then decrease with the further increase of the density. In the dispersion-strengthened coppers similar behaviors were observed as shown in Fig. 11.

In these cases expansion coefficients of dispersion-strengthened irons can be

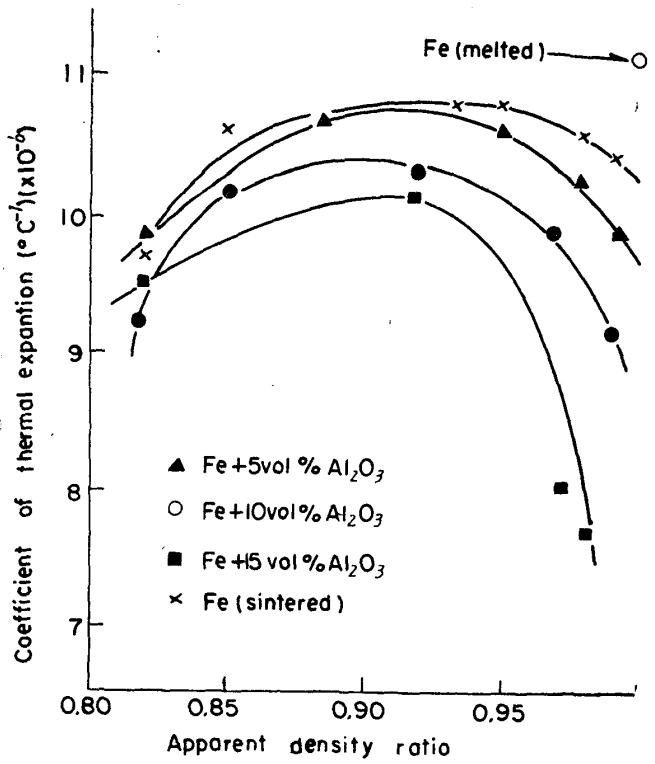

Fig. 10. Relation between coefficient of thermal expansion and apparent density ratio of dispersion-strengthened irons.

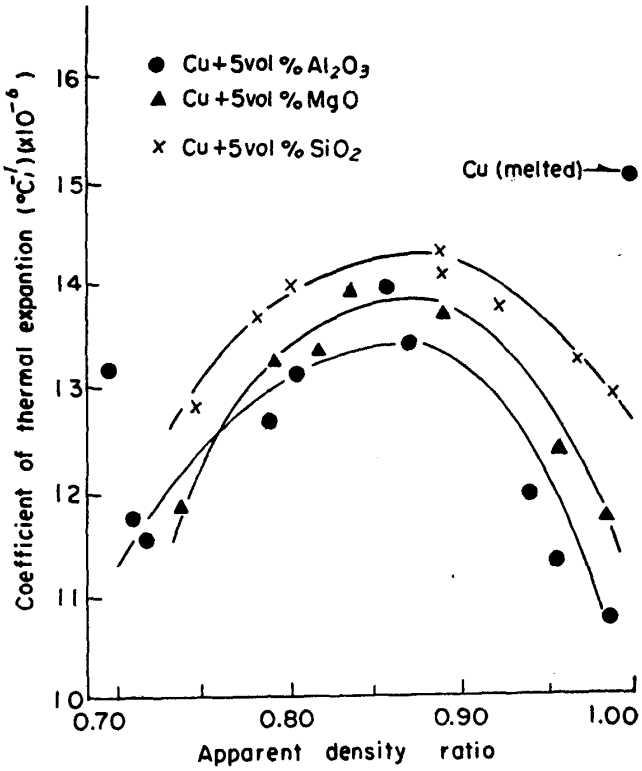

Fig. 11. Relation between coefficient of thermal expansion and apparent density ratio of dispersion-strengthened coppers.

expressed approximately by that of pure iron. For example, in dispersion-strengthened alloy containing 10 vol. per cent of oxide the coefficient α of total thermal expansion is given by

$$\alpha_{total} = \frac{9\,\alpha_{metal}}{10} + \frac{\alpha_{oxide}}{10},$$

where α_{total} and α_{oxide} are coefficients of thermal expansion of iron and oxide, respectively. As α_{metal} is the order of 10^{-5} and α_{oxide} is the order of 10^{-6}, the total expansion coefficient α_{total} is approximately equal to $9\alpha_{metal}/10$, that is,

$$\alpha_{metal} = \frac{10\,\alpha_{total}}{9}$$

The coefficients, α_{metal}, obtained from this calculation are shown in Figs. 9 and 10.

It may be ture that the difference between α_{metal} calculated and the expansion coefficient of melted pure metal, viz. $\alpha_{Fe}=11.2\times10^{-6}$ and $\alpha_{Cu}=15.1\times10^{-6}$, is due to the obstruction of thermal expansion of matrix by dispersed particles.

The maximum expansion coefficient in Figs. 10 and 11 may be considered as follows: In a sintered alloy with a small density the thermal expansion is partially absorbed by porosities, while as the density exceeds a certain value the thermal expansion is obstructed by dispersed particles, and therefore, a maximum coefficient is observed at the density ratio about 0.90.

The obstruction of thermal expansion may be due to the difference of coefficients of base metal and dispersed oxide. From these results, a relation between the thermal expansion and the softening by annealing of cold-worked specimens will be seen: the smaller the expansion is, the less the softening of the dispersion alloys at heating up to a temperature above recrystallization point of base metal. For example, (1) The larger the expansion coefficients of three alloys shown in Fig. 11 are, the more these alloys are softened as shown in Fig. 4; (2) In alloys with the density ratio above 0.90, the higher the density is, the smaller the expansion coefficient is as shown in Figs. 10 and 11. This is in order of softening of dispersion-strengthened irons by annealing above recrystallization temperature; (3) Moreover, the difference between the expansion coefficients of a dispersion-strengthened alloy and melted metal is generally larger in copper base than in iron alloys as shown in Figs. 10 and 11. This corresponds to the larger softening in iron base alloys than in copper base alloys as shown in Fig. 12, which shows the change in annealing hardness of the dispersion-strengthened iron and copper with nearly equal density.

Thus, it may be remarked that a relation exists between the thermal expansion and the softening of dispersion-strengthened alloys.

Fig. 13 shows dilatometric curves of dispersion-strengthened copper and iron and pure melted copper. The dispersion-strengthened alloys showed less contraction at temperatures below about 400°C on cooling from a high temperature as

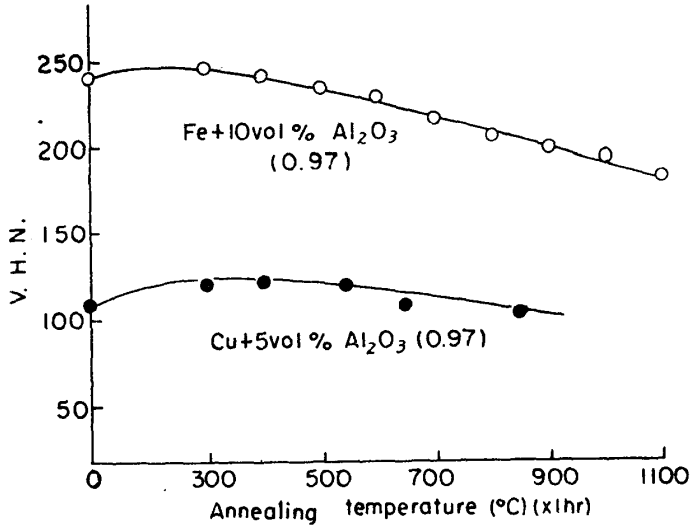

Fig. 12. Change of annealing hardness of iron base and copper base dispersion-strengthened materials.

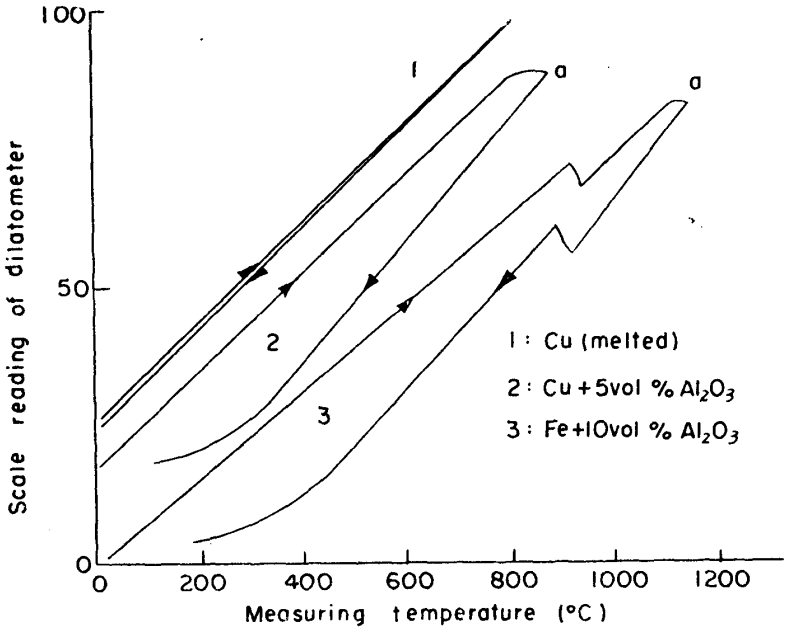

Fig. 13. Difference of dilation curves between the dispersion-strengthened iron and copper and the ordinary melted copper.

shown in curves 2 and 3. This is not due to any experimental error, because in melted copper the contraction was linear as shown in curve 1.

At 300～400°C pure iron and copper have no phase transformation and also no chemical reaction takes place between matrix and alumina, and hence the decrease of contraction may be due to the obstruction by oxide particles. When an alloy which contains dispersed material having smaller thermal expansion is cooled from a high temperature, it is expected that the stress around dispersed

particles caused by the difference of expansion coefficients between the matrix and the dispersed phase obstructs the contraction of the matrix, and consequently, the total contraction of specimen will decrease. However, it cannot be concluded that the cause of the suppression of thermal contraction or expansion is due only to the difference between expansion coefficients of metals and oxide, since as shown in Fig. 11 the alloy containing silica showed a larger expansion coefficient than that of alloy containing alumina of magnesia.

Recently, Ashbey and Smith have shown a stress filed caused by the difference in expansion coefficients by observing electronmicrograph of Cu-SiO_2 alloy prepared by internal oxidation.[12] On Cu-Al_2O_3 alloy, however, they said that stress field in this alloy was produced by the coherency at the interfaces of copper matrix and alumina particles.

It may be not at all for the cause of dispersion-strengthening of Fe-Al_2O_3 alloy in the present work, since the alloy was obtained by mechanical mixing of iron powder and alumina, while the above Cu-Al_2O_3 alloy was obtained by internal oxidation. However, from the facts that Fe-Al_2O_3 alloys have a larger strain field caused by a smaller thermal expansion, and a superior mechanical property, it may be inferred that Fe-Al_2O_3 alloys have superior chemical bond in the interfaces of matrix and oxide particles.

In the present work, the thermal expansion and the hardness measurements for cold-worked specimen were carried out with specimens of different states, that is, the former with sintered specimens and the latter with cold-worked ones (Figs. 1 and 10). Therefore, it cannot be inferred a physical relationship from the present results. However, from the experimental results it may be considered that the thermal interference of particles with matrix and the chemical interaction between oxide and matrix affect the thermal expansion of the alloy and the softening of cold-worked specimens.

Acknowledgements

The authors are grateful to Mr. N. Kagawa who aided us throughout this work. Further thanks are due to Tohoku Metal Co. Ltd. for the kind cooperation.

(12) M.F. Ashbey and G.C. Smith, J. Inst. of Metals, **91** (1963), 182.